ChemComm

COMMUNICATION

View Article Online
View Journal | View Issue

Cite this: *Chem. Commun.*, 2015, 51, 16072

Received 6th July 2015,
Accepted 7th September 2015

DOI: 10.1039/c5cc05546f

www.rsc.org/chemcomm

Magnetic anisotropy of iron-based metallic glassy fibers†

Weibing Liao,[a] Yinshan Meng,[b] Ming Xu,[a] Jiaxin Zheng,[a] Song Gao*[b] and Feng Pan*[a]

Flexible, uniform and surface smooth iron-based metallic glassy fibers (MGFs) were fabricated by a melt-extraction method. There was large magnetic anisotropy in the MGF. Our experimental results indicated that this large magnetic anisotropy was related to the unique magnetic domain structures in the MGF.

Iron-based and cobalt-based metallic glassy fibers (MGFs) are of commercial interest[1–4] due to their intriguing magnetic properties including the giant magneto-impedance effect,[5,6] giant stress-impedance,[7,8] large Barkhausen effect[9] and Matteucci effect,[10] which have been employed in some micro-electro-mechanical system (MEMS) applications. However, various issues regarding the application of MGFs as MEMSs are still unclear and are yet to be solved, such as the magnetic domain microstructures and the magnetic performance along different magnetization directions. Systematic studies of the magnetic domain structures and the intrinsic magnetic properties of MGFs would definitely shed new insights into their magnetization mechanisms. In this communication, we investigated the widely commercially used iron–silicon-based magnetic MGFs,[3–6] such as Fe–Si–B, to be doped with Cr to protect oxidation. The $Fe_{74.5}Si_{10}B_{12}Cr_{3.5}$ was demonstrated to show remarkable magnetic properties using a magnetometer and magnetic force microscopy (MFM). Interestingly, it is also found that the MGF has structural isotropy but magnetic anisotropy, which was closely correlated with the unique structure of the MGF.

Alloy ingots with a nominal composition of $Fe_{74.5}Si_{10}B_{12}Cr_{3.5}$ were prepared by arc-melting a mixture of elements with a purity level of >99.9% in a Ti-gettered high purity argon atmosphere. Minor addition of Cr is to improve the glass forming ability and corrosion properties of the alloy. The cylindrical rods with a diameter of 8 mm were prepared by copper-mold casting under an argon atmosphere. Then the fibers were prepared by the melt-extraction method. The details of MGF preparation can be referred to as given in ref. 11 and the ESI.† The surface morphologies and actual fiber diameters were examined using a scanning electron microscope (SEM). Magnetic measurements were performed using a Quantum Design MPMS-XL5 SQUID magnetometer. Samples were fixed in the capsule. The capsule used in magnetic measurement is made of gelatin with the size of height: 7 mm; diameter: 5 mm. The diamagnetic contribution from the sample holder was measured from 2 to 300 K, with the value of 1.4×10^{-8} emu Oe^{-1}. The fiber with a length of 5 mm was fixed on the sample holder by low temperature kapton tape. The fiber was first put parallel to the applied magnetic field to take parallel measurement, and then put perpendicular to the applied magnetic field to take the perpendicular measurement. The parallel and perpendicular measurements were conducted separately. The magnetization *versus* field data were collected between −5 T and 5 T, with an average field-scanning rate of 0.19 mT s^{-1}. Surface magnetic force morphology and domain structures were investigated using magnetic force microscopy (MFM) (Bruker Nanoscope V System with Multimode 8) at room temperature.

Fig. 1a shows the outer appearance of the melt-extracted $Fe_{74.5}Si_{10}B_{12}Cr_{3.5}$ MGFs. All the fibers are continuous and highly flexible with a diameter of about 50 μm. Excellent surface smoothness and high uniformity can been seen in the magnified image of the MGFs (Fig. 1b). Spectroscopy analysis shows that there is no oxide layer on the surfaces of the MGFs. Fig. 1c shows the typical example of the micrograph of the transverse cross section of the MGFs, and high quality fibers with uniform and perfect circular cross sections can be observed.

Fig. 2 shows the comprehensive magnetic properties of the $Fe_{74.5}Si_{10}B_{12}Cr_{3.5}$ MGFs in longitudinal and horizontal directions. The results of measuring the longitudinal and horizontal hysteresis *M–H* loops at 2 K and room temperature are shown in Fig. 2a and b, respectively. From Fig. 2a, it can be obviously seen that the saturation magnetizations M_s of the

[a] *School of Advanced Materials, Peking University, Shenzhen Graduate School, Shenzhen 518055, China. E-mail: panfeng@pkusz.edu.cn*
[b] *College of Chemistry and Molecular Engineering, Peking University, Beijing 100871, China. E-mail: gaosong@pku.edu.cn*

† Electronic supplementary information (ESI) available: Experimental procedure and additional data. See DOI: 10.1039/c5cc05546f

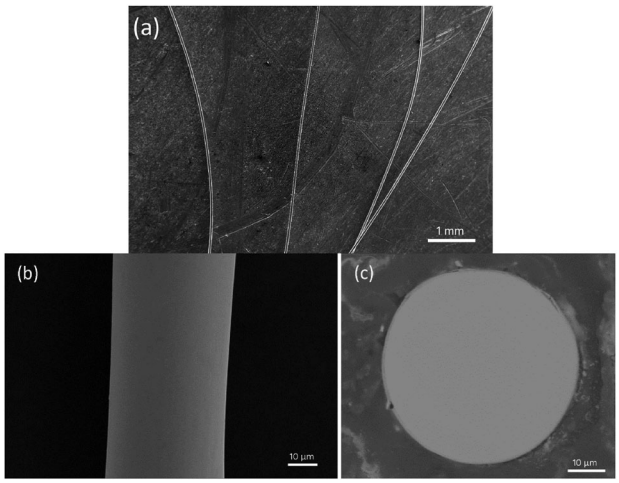

Fig. 1 (a) Outer appearance of the melt-extracted fibers of $Fe_{74.5}Si_{10}B_{12}Cr_{3.5}$ alloy, (b) the magnified morphology of (a), and (c) the typical morphology of the cross section shape of the fiber.

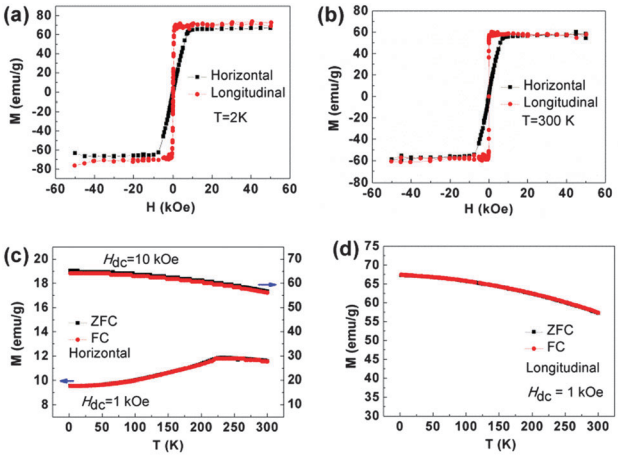

Fig. 2 Magnetic hysteresis loops measured at a maximum applied field of 5 T for the $Fe_{74.5}Si_{10}B_{12}Cr_{3.5}$ MGFs from the longitudinal and horizontal directions (a) at 2 K and (b) at 300 K, and temperature dependence of magnetization-$M(T)$ curves, (c) from the horizontal direction and (d) from the longitudinal direction.

MGFs tested along the longitudinal and horizontal directions at 2 K are nearly the same (Table 1), but the applied magnetic field strength to reach the saturation magnetization point (H_s) from the longitudinal direction is 0.75 kOe, which is much smaller than 8.32 kOe from the horizontal direction. Even at room temperature the MGFs possess almost the same features as shown in Fig. 2b. The data are summarized in Table 1. These results indicate that the MGF has structural isotropy but magnetic anisotropy, and its easy magnetization direction is from the longitudinal side. The low coercive force H_c of the MGF listed in Table 1 is considered to be related to the microstructures of the MGFs. As in the metallic glassy state, the MGFs lack the long range order (crystalline structure), but possess homogeneous microstructures without any grain boundaries or large chemical precipitates.[12] As a result, the defects are very narrow for pinning

Table 1 The comparison of the magnetic properties of the $Fe_{74.5}Si_{10}B_{12}Cr_{3.5}$ MGF tested from the longitudinal direction and horizontal direction. Saturation magnetization M_s, coercive force H_c, and applied magnetic field strength to reach the saturation magnetization point H_s

	Longitudinal at 2 K	Horizontal at 2 K	Longitudinal at 300 K	Horizontal at 300 K
M_s (emu g^{-1})	68.2	66	57.33	54.6
H_c (A m^{-1})	5	10	14	33
H_s (kOe)	0.75	8.32	0.4	7.5

the movement and rotation of the magnetic domain walls during technical magnetization.

In order to further verify this magnetic anisotropy fact, magnetization measurements as a function of temperature and orientation were performed. The temperature dependence of magnetization-$M(T)$ curves was measured from 2 K to 300 K parallel and perpendicular to the applied magnetic field of 1 kOe as shown in Fig. 2c and d, respectively. With respect to curves $M(T)$ measured from the horizontal and longitudinal directions, the zero-field-cooled (ZFC) curves coincide much well with the field-cooled (FC) curves, but the $M(T)$ value tested along the longitudinal direction is 65–56 emu g^{-1}, which is much larger than that along the horizontal direction, about 10–13 emu g^{-1}. These data reveal that the MGF is magnetized much more easily from the longitudinal direction, further confirming that the MGF has magnetic anisotropy. It is worth noting that the MGF possessed a weak broad peak at about 225 K, as shown in the $M(T)$ curve in Fig. 2c, and this event verified that there was an antiferromagnetic order in the MGF. This broad peak would disappear when the MGF reaches saturation magnetization. The M along the horizontal direction at 10 kOe and along the longitudinal direction at 1 kOe of the MGF continuously decreases with increasing temperature, because it is mainly related to the thermal vibrations of the atoms. Thus, it is apparent that the steep response around the original point of Fig. 2a observed along the horizontal direction includes spin-flip transition behaviour (Fig. S2, ESI†). Furthermore, the M is initially proportional to the applied magnetic field H in the paramagnetic phase at 300 K along the horizontal direction (Fig. 2b). Then it will become saturated at the saturation magnetization point H_s, forming the S-shaped curve. As there is superexchange interaction at 2 K, the value of H_s is a little bigger than that at 300 K along the horizontal direction (Table 1)

Magnetic force microscopy (MFM) measurements were conducted to further identify the surface magnetic domain microstructure distribution. A typical selected area of the MGF with a scanning size of 10 × 10 μm^2 by MFM was fixed (marked by A), as indicated in Fig. 3a. Fig. 3b shows the surface height morphology of the A area, which further confirms that the melt-extracted MGFs have a smooth surface. In Fig. 3c, it can be observed that there is a distinct colour contrast in the micron-sized MGFs, distinguishing the features of alternate "dark" and "bright" magnetic domain structures with a width of about 1–2 μm. This suggests a strong magnetic anisotropy with the magnetic easy axis normal to the plane of the sample. As the magnetization is along the easy axis and normal to the plane of

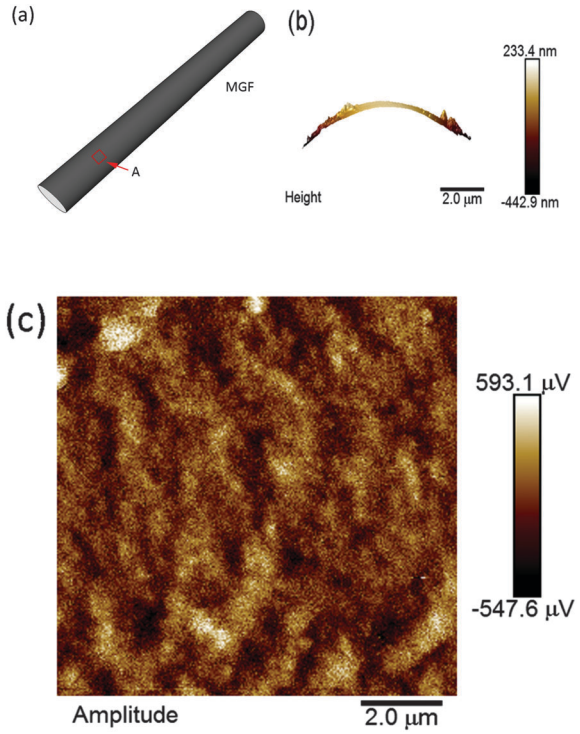

Fig. 3 Surface MFM images of the $Fe_{74.5}Si_{10}B_{12}Cr_{3.5}$ MGFs with a scanning size of 10 μm × 10 μm. (a) The selected area on the MGF denoted by A, (b) the 3D surface height image, and (c) the 2D surface magnetic force image.

the sample, ''dark'' and ''bright'' magnetic domain structures were formed so that the demagnetization field would be reduced. These ''dark'' and ''bright'' structures also demonstrate that the magnetization direction coexists in and out of the surface of the fibers, indicating that radial magnetic domain structures were formed. Even though the MGFs are amorphous and thin, the MFM results reveal its complex domain structures on the surface.

Based on the above experimental results, the domain structures distributed in the iron-based MGF can be proposed in Fig. 4. The MGF possessed a ''core–shell'' domain structure consisting of a large internal domain with magnetization lying along the fiber axis and covered by the external domain structure with radial magnetized domains. The difference between the magnetic domains in the core and in the shell results in the magnetic anisotropy of the MGF. In fact, many studies showed that the magnetic domain structures were related to the residual stress in the MGF.[5,13,14] In previous studies,[13,15,16] the MGF was glass-coated and the difference in the coefficients of thermal expansion of glass and metal would lead to high radial stresses, which were maximal at the metallic core surface and decreased sharply toward the wire axis. The presence of such a residual stress field led to the formation of a complex magnetic structure. However, in our study the MGF was exposed without any coverings, thus the resultant residual stress field was mainly induced during the fabrication of amorphous microfibers. As the MGF was prepared by the melt-extraction method, axial tension stresses and quenching stresses related to the temperature gradient occurring in the metal upon quenching could be highly expected, and the anisotropic ''core–shell'' magnetic domain structures were formed. On the other hand, the asymmetric ''shell'' structure of the MGF may generate the antiferromagnetic order due to differences in the steric and electronic structures on the surface and near the surface of the ''shell'' area, which can lead to unique physical properties around these domain regions. These unique domain structures lead to its magnetic anisotropy, excellent physical properties and would bring about its application as a new engineering and functional material intended for parts of inductive components (*e.g.* high performance magnetic sensors, electromagnetic interference shielding, MEMS, and other applications).

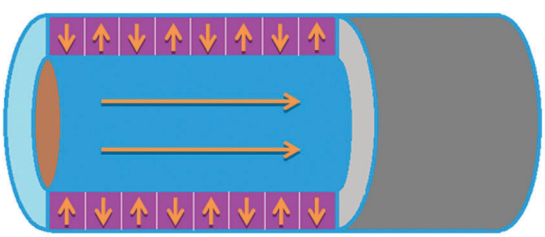

Fig. 4 Schematic domain structures of metallic glassy fibers.

In summary, we reported a benign approach to detect the magnetic structures of the micron-sized $Fe_{74.5}Si_{10}B_{12}Cr_{3.5}$ MGFs and find that there is large magnetic anisotropy, which is related to the magnetic domain structures in the MGFs. The unique domain structures distributed on the surface of the MGFs are revealed by inhomogeneous magnetic force morphology. This would be a paradigm shift in magnetization technology because the surface domain structure characterization is a key issue for designing and building reliable and high-performance magnetic sensors and devices. As-prepared micron-sized MGFs associated with excellent flexibility, easy handling, low coercive force and high saturation magnetization will find broad industrial applications. In addition, this work could open new opportunities for using active multi-element metallic systems to functionalize more flexible micron-sized metallic fibers with better magnetic performance.

This work was supported by the Guangdong Innovation Team Project (No. 2013N080) and the Shenzhen Science and Technology Research Grant (No. ZDSY20130331145131323).

Notes and references

1 Y. Wu, H. X. Li, G. L. Chen, X. D. Hui, B. Y. Wang and Z. P. Lu, *Scr. Mater.*, 2009, **61**, 564.
2 Y. Wu, H. H. Wu, X. D. Hui, G. L. Chen and Z. P. Lu, *Acta Mater.*, 2010, **58**, 2564.
3 H. Wang, F. X. Qin, D. W. Xing, F. Y. Cao, X. D. Wang, H. X. Peng and J. F. Sun, *Acta Mater.*, 2012, **60**, 5425.
4 F. X. Qin and H. X. Peng, *Prog. Mater. Sci.*, 2013, **58**, 183.
5 H. Chiriac and T. A. Ovari, *Prog. Mater. Sci.*, 1996, **40**, 333.
6 M. Vazquez, *J. Magn. Magn. Mater.*, 2001, **226**, 693.
7 D. R. Li, Z. C. Lu and S. X. Zhou, *Sens. Actuators, A*, 2003, **109**, 68.
8 J. F. Hu, H. W. Qin, J. Chen and Y. Z. Zhang, *J. Magn. Magn. Mater.*, 2003, **266**, 290.
9 J. Gonzalez, N. Murillo, V. Larin, J. M. Barandiaran, M. Vazquez and A. Hernando, *Sens. Actuators, A*, 1997, **59**, 97.

10 P. D. Dimitropoulos and J. N. Avaritsiotis, *Sens. Actuators, A*, 2001, **94**, 165.
11 W. B. Liao, J. M. Hu and Y. Zhang, *Intermetallics*, 2012, **20**, 82.
12 M. W. Chen, *Annu. Rev. Mater. Res.*, 2008, **38**, 445.
13 N. N. Orlova, A. S. Aronin, S. I. Bozhko, Yu. P. Kabanov and V. S. Gornakov, *J. Appl. Phys.*, 2012, **111**, 073906.
14 H. Chiriac, T. A. Ovari and G. Pop, *Phys. Rev. B: Condens. Matter Mater. Phys.*, 1995, **52**, 10104.
15 M. Vazquez and A. P. Zhukov, *J. Magn. Magn. Mater.*, 1996, **160**, 223.
16 R. Varga, A. Zhukov, J. M. Blanco, M. Ipatov, V. Zhukova, J. Gonzalez and P. Vojtanik, *Phys. Rev. B: Condens. Matter Mater. Phys.*, 2006, **74**, 212405.